Temporally resolved cavity ring-down spectroscopy in a pulsed nitrogen plasma

A. P. Yalin[a] and R. N. Zare
Department of Chemistry, Stanford University, Stanford, California 94305

C. O. Laux and C. H. Kruger
Department of Mechanical Engineering, Stanford University, Stanford, California 94305

(Received 23 January 2002; accepted for publication 19 June 2002)

Cavity ring-down spectroscopy (CRDS) has enabled temporally resolved measurements of the N_2^+ ion concentration in a pulsed atmospheric pressure nitrogen plasma. A 10 ns voltage pulse is applied to a dc-sustained plasma to change the ionization fraction rapidly. Our measurements show that the pulse increases the N_2^+ ion concentration from 3.9×10^{12} to more than $1.5\times10^{13}\ \mathrm{cm}^{-3}$, and that the N_2^+ concentration returns to the dc level in about 10 μs. We also determine the electron density by measuring the electrical conductivity of the plasma. Because N_2^+ is the dominant ion, the good agreement between electrical and CRDS measurements provides validation of the temporally resolved CRDS technique. [DOI: 10.1063/1.1500427]

Pulsed plasmas are of growing interest in many plasma-processing applications, including etching, deposition, surface modification, and biochemical decontamination. Ion concentration and electron number density are key parameters in the analysis and optimization of such systems, but their measurement often poses considerable difficulty. Here, we report the use of CRDS to perform temporally resolved measurements of the N_2^+ ion concentration in a pulsed atmospheric pressure nitrogen discharge.

Cavity ring-down spectroscopy (CRDS) has become a widely used method in absorption spectroscopy.[1] Briefly, a pulsed laser beam is coupled into a high-finesse optical cavity containing a sample, where it passes many times between the mirrors. As the light bounces back and forth inside the cavity, its intensity decays (rings down) owing to sample absorption and cavity loss (caused primarily by mirror reflectivity). A photodetector is used to measure the ring-down signal, which is fit to yield the sample loss. The technique enables measurements of weakly absorbing and/or low concentration species owing to a combination of long effective path length and insensitivity to laser energy fluctuations. Previously, CRDS has been applied to measure the concentrations of ions in dc plasmas.[2–5] Here, we use the CRDS technique to study dynamic processes in evolving plasmas.

Figure 1 shows a photograph of the atmospheric pressure nitrogen discharge, as well as a schematic diagram of the CRDS setup. Nitrogen is injected through a flow straightener and passes through the discharge region with a velocity of about 20 cm/s. The discharge is formed between a pair of platinum pins (separation 0.85 cm) vertically mounted on water-cooled stainless steel tubes. The discharge is maintained by a dc current supply (187 mA) in a ballasted circuit ($R_b=9.35\ \mathrm{k}\Omega$). We study the N_2^+ ion by probing the (0,0) band of its first negative system ($B^2\Sigma_u^+-X^2\Sigma_g^+$) in the vicinity of 391 nm. We select this spectral feature because it is comparatively strong and optically accessible. An optical parametric oscillator (OPO) system (doubled idler) is used as the light source (pulse width ~7 ns, pulse energy ~1 mJ, linewidth ~$0.14\ \mathrm{cm}^{-1}$). A 75 cm cavity yields typical ring-down times of approximately 10 μs, corresponding to mirror reflectivities of about 0.99 975. The plasma has strong thermal gradients that tend to steer the beam and destabilize the cavity.

We find that appropriate selection of cavity geometry is critical to implementation of the CRDS technique.[6] The results reported here use 50 cm radius-of-curvature mirrors and a 75 cm length linear cavity. To obtain a spatial profile of the N_2^+ concentration in the dc sustained plasma, we displace the discharge perpendicularly to the optical axis. CRDS is a path-integrated technique and the discharge has axial symmetry, which we verify by performing measurements with the plasma rotated by 90° (<2% deviation). We use an Abel inversion to recover the radial N_2^+ concentration profile. The dc concentration measurement is based on the (wavelength integrated) area of the lines P(9)–P(17). The inverted data for the dc plasma yield the radial profile of ion concentration shown in Fig. 2, which has a centerline (peak) concentration of $3.9\pm0.6\times10^{12}\ \mathrm{cm}^{-3}$, and half-maximum of concentration at radius 1.04 ± 0.03 mm. The error bars (1σ) on N_2^+ concentration primarily arise from uncertainty in relating the measured absorbance (which corresponds to the population of several rotational levels in the ground vibronic state) to the overall population of N_2^+. Boltzmann plots of the rotational lines yield a rotational temperature of 5600 ± 400 K at the center of the discharge, and 4700 ± 300 K at the radial

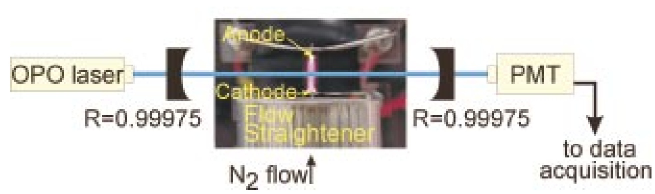

FIG. 1. (Color) Photograph of the atmospheric pressure nitrogen discharge and schematic diagram of the CRDS setup. The electrode separation is 0.85 cm, and a current of 187 mA passes through the discharge. An OPO is used as the light source, and a photomultiplier tube detects the light exiting the cavity.

[a]Electronic mail: azer@saha.stanford.edu

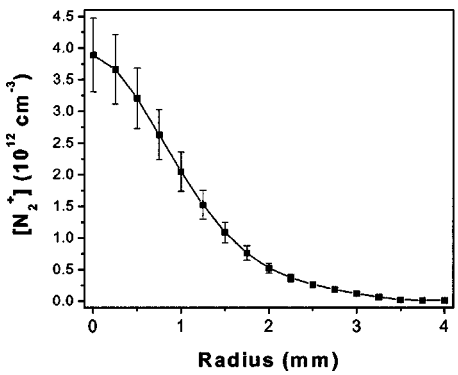

FIG. 2. Radial profile of N_2^+ ion concentration in dc discharge found by CRDS.

half-maximum of ion concentration. The rotational temperature is close to the gas temperature owing to fast collisional relaxation at atmospheric pressure. A collisional-radiative model[7] is used to determine the fraction of the population in the ground electronic and ground vibrational state, and predicts 0.73 ± 0.08 and 0.41 ± 0.04, respectively. Combining these uncertainties with the uncertainty from the Abel inversion (~4%) results in an overall experimental uncertainty of 15%.

To increase the time-averaged concentration of charged species in the nitrogen plasma, we investigate the use of short, high voltage pulses. Although a number of kinetics studies have been performed with CRDS, nearly all of these experiments study processes that are slow compared to experimental ring-down times. An exception is the work of Brown *et al.*,[8] who perform gas-phase measurements in cases in which the populations do change over the duration of the ring-down. For the case of a time-dependent absorption, the ring-down signal $S(t)$ may be written as:[8]

$$S(t)=S_0 \exp\left\{-(c/L)\left[\int_0^t k(\nu,t) l_{\mathrm{abs}} dt+(1-R)t\right]\right\}, \tag{1}$$

where S_0 is the signal at time zero, L is the cavity length, c is the speed of light, k is the absorption coefficient, l_{abs} is the path length of absorber, and $1-R$ is the effective empty cavity loss. Rearranging Eq. (1) leads to an expression for the absorbance as a function of time:

$$\mathrm{Abs}(t) \equiv k(\nu,t) l_{abs}=(-L/c)\frac{d}{dt}\{\ln[S(t)/S_0]\}-(1-R). \tag{2}$$

The derivative (local slope) of the logarithm of the ring-down signal is proportional to the loss (sample plus empty cavity) at that time. To directly obtain time-dependent concentrations, we divide the ring-down signal into a series of time-windows, and in each window we fit a line segment (slope) to the logarithm of the signal. It might be tempting to consider using lower reflectivity mirrors with shorter ring-down times so that the losses may be treated as constant over the ring-down, but the sensitivity of such an approach is inferior.[1]

We create a pulsed discharge by coupling a high-voltage pulser in parallel to the dc discharge circuit. The dc field serves to give a baseline of ionization and to heat the gas. We

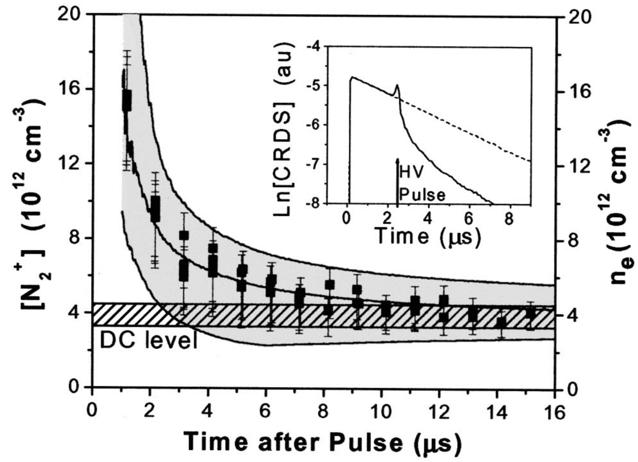

FIG. 3. CRDS measurements of N_2^+ concentrations (squares) and conductivity measurements of electron densities (line and swath) versus time following the firing of a high-voltage pulse in an atmospheric pressure nitrogen dc plasma. The inset shows experimental ring-down traces with the high-voltage pulse (solid line) and without the high-voltage pulse (dashed line).

operate the high-voltage pulser (pulse width ~10 ns, pulse voltage ~8 kV) at ~10 Hz so that it may be synchronized relative to the laser. At this repetition rate the plasma completely recombines between high-voltage pulses so that the behavior during and following each pulse is not affected by the presence of other pulses. Because the pulse length is short compared to our time resolution, we do not resolve the buildup of ionization; yet we are able to resolve the subsequent recombination.

The inset in Fig. 3 shows ring-down traces obtained with and without firing the high-voltage pulse, with the laser tuned to the N_2^+ bandhead [P(12)–P(14)]. In the absence of the high-voltage pulse (dashed line) the absorption losses are constant in time, and the signal decays as a single exponential. In the trace with the pulse (solid line), the light decays more steeply after the pulse, reflecting an increased concentration of N_2^+ . The spike in the latter trace coincides with the firing of the pulse, and is caused by electromagnetic pick-up generated by the pulser. To verify that we are observing changes in the N_2^+ concentration, we examine the analogous traces but with the laser detuned from the absorption band. These traces are identical to one another (except for in the vicinity of the electromagnetic pick-up) and confirm that the only effect of the high voltage pulse on the ring-down system is to generate the pick-up spike. From these traces, we determine that the pick-up prevents us from analyzing data in the first 0.7 μs following the firing of the pulse. We vary the delay of the high-voltage pulse relative to the laser shot so that we can obtain ion concentrations at different times.

We quantify the time-varying N_2^+ concentration (at the discharge center) using Eq. (2) with a 1 μs window. This time interval represents a good compromise in making the window short compared to the time scale of the process studied yet affording an acceptable signal-to-noise level. We use the measured mirror reflectivity (found with the laser detuned) and tabulated linestrengths.[9] Owing to the path-integrated nature of CRDS, the measured concentrations are inversely proportional to the assumed path length. As discussed later, the path length of our pulsed discharge may vary by up to a factor of about 1.5 during the measurement.

Figure 3 shows absolute N_2^+ concentrations (squares) obtained using the path length from the measured dc profile (Fig. 2), with error bars that include contributions owing to the uncertainty in path length. To determine the uncertainty in path length, we provide a simplified analysis of the evolution of the concentration profile. For sufficiently long times after a pulse (and therefore just before a subsequent pulse), the profile equilibrates to the dc case. During a high-voltage pulse, ions are predominantly formed by electron impact ionization, according to $[N_2^+](t) \approx [N_2^+](t=0)\exp(k[N_2]t)$, where k is the rate constant for electron impact ionization, and we have assumed $[N_2^+] \approx [n_e]$. According to this expression, the shape of the ion profile immediately after a high-voltage pulse is also the same as in the dc case (but with higher amplitude). The dominant loss mechanism during the recombination phase is dissociative recombination, which tends to broaden the profile (because higher concentrations nearer the center recombine more quickly). Based on these assumptions, we simulate the temporal evolution of the concentration profile, and compute the effective path length as a function of time. Immediately after a high-voltage pulse, we take a profile with the dc shape and amplitude consistent with our CRDS measurement. We then compute the evolution, by assuming to a good approximation, that at each radial location the concentration decays by dissociative recombination until it reaches the level of the dc profile. We use a rate coefficient for dissociative recombination for N_2^+ of 4×10^{-8} cm^3/s from Park.[10] We find that the largest change in the shape of the profile occurs at about 5 μs after the pulse, and corresponds to an increase in effective path length of about 50% (relative to the shape of the dc profile). The uncertainty associated with the path length is smaller at earlier and later times, since the profile shape is closer to the dc case. The downward error bars in Fig. 3 contain contributions due to variations in profile shape. The uncertainty due to the population fractions and other factors are the same as in the dc case, and are also included in the error bars.

We also determine the electron concentration at the center of discharge by measuring the electrical conductivity of the discharge. We write Ohm's law as $j = i/\text{area} = (n_e e^2/m_e \Sigma \nu_{eh})E$ where ν_{eh} is the average collision frequency between electrons and heavy particles. Because of the low ionization fraction ($< \sim 10^{-5}$), ν_{eh} is dominated by collisions with neutrals, so we can write $\nu_{eh} = n_n g_e Q_{en}$, where $n_n = P/kT_g$ is the number density of neutrals, $g_e = (8kT_e/\pi m_e)^{0.5}$ is the thermal electron velocity, and Q_{en} is the average momentum transfer cross section for electron–nitrogen collisions, for which we use $Q_{en} = Q(e\text{-}N_2) = 1.2 \pm 0.2 \times 10^{-15}$ cm^2 from Ref. 11. We determine T_e with a collisional radiative model[7] and obtain a dc value of $T_e = 9500 \pm 500$ K at the radial half-maximum. The dc electric field is found from the slope of discharge voltage versus electrode separation (intercept gives cathode fall). The time dependent electric field is found (after subtracting the cathode fall) from the discharge voltage, which we measure using fast probes (time response$\sim$3 ns). For the dc plasma, we find that the ratio of the area-integrated N_2^+ concentration (from CRDS) to the area-integrated electron concentration (from conductivity measurements) is 0.87 ± 0.25. This result agrees with the prediction of our collisional-radiative model that approximately 85% of ions are N_2^+ and the remainder is N^+. The uncertainty in the dc electron concentration is primarily due to uncertainties in the dc discharge area (5%), electric field (3%), the momentum transfer cross section (17%), and the average gas temperature (15%). The temporally resolved electron concentrations are shown with a solid line in Fig. 3. At early times, the uncertainty in the time-varying electron concentrations is highest, owing to a larger uncertainty in the electric field. (The subtraction of the cathode fall becomes increasingly inaccurate as the cathode fall increasingly dominates the discharge voltage at early times.) The solid line assumes a constant profile shape based on the dc measurement. Extracting the electron concentration from the area-integrated electrical measurement is also sensitive to variation in the shape of the profile. We gauge the magnitude of this effect by computing the effective areas of the simulated profiles discussed previously. The downward portion of the electron number density swath includes uncertainty due to uncertainty in the shape of the profile. The collisional-radiative model predicts that N_2^+ is the dominant ion produced by the pulse. The agreement between the time-dependent electron and N_2^+ concentrations during plasma recombination verifies the CRDS measurement. The experimental recombination time is consistent with reported[10] dissociative recombination rate coefficients for N_2^+.

We have demonstrated the use of the CRDS technique to obtain spatially and temporally resolved ion concentrations at the ppm level in a hostile plasma environment. We measure ppm level concentrations with microsecond temporal resolution. Fundamentally, the time resolution of the technique is limited by the cavity round-trip time. Shorter cavities with faster detection may be used to study systems that evolve more quickly.

This work was funded by the Director of Defense Research & Engineering (DDR&E) within the Air Plasma Ramparts MURI Program managed by the Air Force Office of Scientific Research (Grant # AF-F49620-97-1-0316), and by the Department of Energy, Basic Energy Sciences (Grant # DE-FG03-92ER14304-A007).

[1] G. Berden, R. Peeters, and G. Meijer, Int. Rev. Phys. Chem. **19**, 565 (2000).
[2] M. Kotterer, J. Conceicao, and J. P. Maier, Chem. Phys. Lett. **259, 1–2**, 233 (1996).
[3] F. Grangeon, C. Monard, J.-L. Dorier, A. A. Howling, C. Hollenstein, D. Romanini, and N. Sadeghi, Plasma Sources Sci. Technol. **8**, 448 (1999).
[4] W. M. M. Kessels, J. P. M. Hoefnagels, M. G. H. Boogaarts, D. C. Schram, M. C. M. van de Sanden, J. Appl. Phys. **89**, 2065 (2001).
[5] J. P. Booth, G. Cunge, L. Biennier, D. Romanini, and A. Kachanov, Chem. Phys. Lett. **317**, 631 (2000).
[6] S. Spuler and M. Linne, Appl. Opt. **41**, 2858 (2002).
[7] L. Pierrot, L. Yu, R. J. Gessman, C. O. Laux, and C. H. Kruger, presented at 30th AIAA Plasmadynamics and Lasers Conference, Norfolk, VA, June 28–July 1 1999, paper 99-3478.
[8] S. S. Brown, A. R. Ravishankara, and H. Stark, J. Phys. Chem. A **104**, 7044 (2000).
[9] F. Michaud, F. Roux, S. P. Davis, A.-D. Nguyen, and C. O. Laux, J. Mol. Spectrosc. **203**, 1 (2000).
[10] C. Park, *Nonequilibrium Hypersonic Aerothermodynamics* (Wiley, New York, 1990), pp. 271–272.
[11] K. Tsang, K. Papadopoulos, A. Drobt, P. Vitello, T. Wallace, and R. Shanny, Radio Sci. **26**, 1345 (1991).